Nonlinear dynamics of higher-order solitons near the oscillatory instability threshold

Kazimir Y. Kolossovski and Alexander V. Buryak
School of Mathematics and Statistics, University of New South Wales, Australian Defence Force Academy, Canberra 2600, Australia

Dmitry V. Skryabin
Department of Physics and Applied Physics, University of Strathclyde, 107 Rottenrow, Glasgow G4 0NG, United Kingdom
and Department of Physics, University of Bath, Bath BA2 7AY, United Kingdom

Rowland A. Sammut
School of Mathematics and Statistics, University College Australian Defence Force Academy, Canberra ACT 2600 Australia
(Received 19 March 2001; published 23 October 2001)

Nonlinear theory describing the dynamics of solitons in the vicinity of oscillatory instability threshold with a low frequency offset is developed. The theory is tested on the example of parametric degenerate four-wave mixing. All major predictions of our theory are in agreement with the results of direct numerical modeling. This includes the position of oscillatory instability threshold, instability rates, and various instability development scenarios.

DOI: 10.1103/PhysRevE.64.056612 PACS number(s): 42.65.Tg, 42.81.Dp, 05.45.Yv

I. INTRODUCTION

Among the most fascinating objects of nonlinear science are solitons—self-guided beams and pulses. One of the reasons for the current interest in optical solitons is due to the possibility of all-optical switching and controlling light by light (see, e.g., [1]). Continuous growth of theoretical knowledge for existence, effective generation, and stability of different types of solitary waves is backed by a variety of successful experiments [2].

Stability of solitons is one of the paramount questions (see e.g., [3] and references therein). The majority of theoretical results related to the dynamics of solitary waves were obtained via *linear* spectral stability analysis. This describes well only the initial stages of perturbed soliton evolution and leaves unresolved its subsequent dynamical behavior. During the last decade several model equations, like generalized nonlinear Schrödinger equation (NLS) [4,5] and three-wave mixing [6,7], were used to develop theory describing longer-term *nonlinear* dynamics of solitons near the Vakhitov-Kolokolov (VK) instability threshold [8]. This theory successfully explains persistent oscillations, decay and collapse of the solitary waves, and transitions between these scenarios [4]. VK instability being a particular example of the instability generated by purely real eigenvalues in the soliton spectrum, is a typical first instability for the fundamental (nodeless) solitary solution.

Higher-order (excited-state) solutions are also of significant fundamental and practical interest. Recently, wide interest in such solitons has been aroused by the discovery of several classes of stable higher-order solitons in different nonlinear media [9,10]. The most typical scenario of instability of the higher-order states is, however, instability due to complex eigenvalues. One of the first examples of complex eigenvalues in the linear spectrum of a Hamiltonian system is associated with the antisymmetric mode of nonlinear planar waveguide, Refs. [11]. For more recent examples of oscillatory instability see Refs. [12]. Analytical treatment of such instabilities is much more involved and one of the first steps in this direction was made in [13], where the general *linear* asymptotic stability analysis capable of capturing complex eigenvalues has been developed, but has not been backed up with any physical example. The approach used in [13] is based on the assumption that oscillatory and VK instabilities happen sufficiently close to each other (in the vicinity of the *codimension two point* where four corresponding eigenvalues merge at zero and the governing eigenvectors coincide). On the other hand, recent numerical studies of the spectral properties of the optical solitons degenerate four-wave mixing (FWM) [10] have revealed the existence of exactly such a point for one of the higher-order soliton families, suggesting that this situation may be much more typical for complex nonlinear evolutional models than previously thought. The goal of this work is a detailed study of this FWM example and nonlinear generalization of the linear theory of Ref. [13]. We derive a nonlinear ordinary differential equation (ODE) model that provides a valuable insight into longer-term instability-induced dynamics of higher-order solitons allowing us to classify different instability development scenarios. All major predictions of our analytic results are in full agreement with direct numerical simulations.

II. DEGENERATE FOUR-WAVE MIXING MODEL

We intend to demonstrate all major steps of the derivation of our nonlinear dynamics theory in the example of a specific physical model representing a degenerate case of parametric FWM in the presence of self- and cross-phase modulation. The equations for this model are

$$\begin{aligned} i\frac{\partial U}{\partial Z}+\frac{\partial^2 U}{\partial X^2}-\beta U+N_1+\frac{1}{3}U^{*2}W=0,\\ i\sigma\frac{\partial W}{\partial Z}+\frac{\partial^2 W}{\partial X^2}-\sigma(3\beta+\Delta)W+N_2+\frac{1}{9}U^3=0, \end{aligned} \tag{1}$$

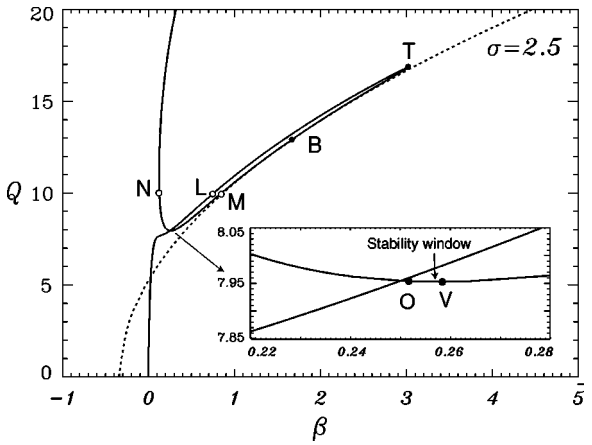

FIG. 1. Soliton families of Eqs. (1) at $\sigma=2.5$. Dashed curve corresponds to the one-wave family ($U=0$, $W\neq 0$); solid curves represent two-wave soliton families. Point *B* shows the position of the bifurcation of two-wave soliton families from the one-wave family separated by a turning point *T*. Insert shows the vicinity of stability window bounded by VK instability (point *V*) and oscillatory instability (point *O*) thresholds.

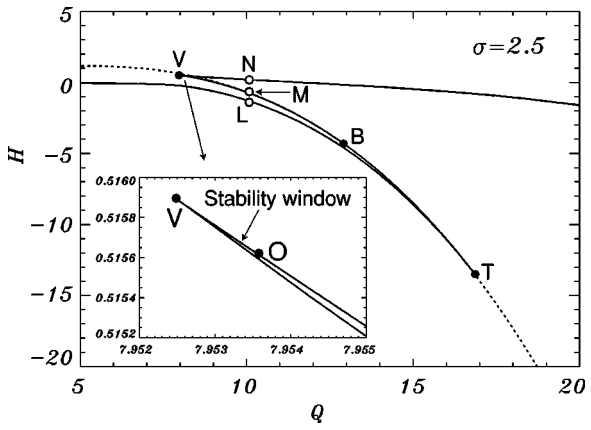

FIG. 2. Hamiltonian versus energy diagram for the soliton families of Eqs. (1). All labeling and notations correspond to the labeling and notations in Fig. 1.

where nonparametric nonlinear terms are expressed by functions $N_1=(|U|^2/9+2|W|^2)U$, $N_2=(9|W|^2+2|U|^2)W$, slowly varying complex functions U and W are amplitudes of the fundamental and the third harmonics, respectively, the parameter β measures the shift in the propagation constant, Δ is the wave-vector mismatch, and Z is the propagation distance. For the spatial soliton case the dimensionless parameter σ is the ratio of the wave numbers of the harmonics and is equal to 3 whereas for the case of the temporal soliton the value of σ can vary. Some special sech-like solitons of this model were found in Refs. [14] whereas the question of families of two-wave solitons was addressed in Refs. [15]. The key property of this model is that it admits the existence of a broad range of different higher-order soliton families including stable, unstable, and oscillatory unstable ones [10].

Equations (1) have three integrals of motion, hamiltonian, energy, and momentum, of which Hamiltonian H and energy Q are important for our analysis. These invariants are given by

$$H=\int_{-\infty}^{+\infty}\left\{\left|\frac{\partial U}{\partial X}\right|^2+\left|\frac{\partial W}{\partial X}\right|^2-\frac{1}{18}|U|^4-\frac{9}{2}|W|^4-2|U|^2|W|^2-\frac{1}{9}(WU^{*3}+W^{*}U^3)+\sigma\Delta|W|^2\right\}dX,$$

$$Q=\int_{-\infty}^{+\infty}\{|U|^2+3\sigma|W|^2\}dX. \tag{2}$$

To present and classify soliton families we use invariants (2) calculated for soliton profiles. Figure 1 shows the dependence of energy Q versus soliton parameter β at $\Delta=1.0$ and $\sigma=2.5$. Corresponding parametric dependence $H=H(Q)$ is presented in Fig. 2. Examples of the representatives of two lowest-order two-wave soliton families are given in Fig. 3.

Note, that for any $\Delta>0$ the corresponding diagrams may be easily obtained by an appropriate scaling transformation.

The analysis of Ref. [10] identified that fundamental two-wave soliton family (the lowest in *H*-*Q* diagram, which goes up to a point *T* in Figs. 1 and 2) is always stable in the whole domain of existence (for any fixed $\Delta>0$ and $\sigma\simeq 3$). At the turning point *T* solitons lose their stability and the emerging higher-order soliton family is unstable until VK stability threshold (point *V*), where surprisingly it does not acquire the second instability mode, but *regains* stability in a small range of the parameter β, before losing it again due to oscillatory instability (point *O*). Varying σ one can find the codimension two point, where the stability window exactly vanishes, the eigenvectors driving both instabilities coincide, and all formal conditions for the theory presented below are

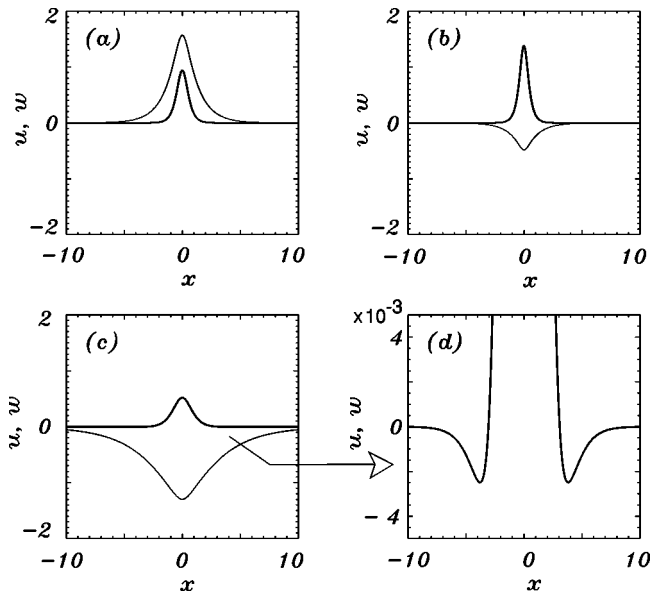

FIG. 3. Examples of soliton profiles at energy level $Q=10$. The profiles shown in plots (*a*), (*b*), and (*c*) correspond to the points *L*,*M*, and *N* in Figs. 1 and 2. Figure (*d*) is enlarged fragment of the plot (*c*). Note nonmonotonic soliton tails — a distinctive feature of higher-order solitons.

satisfied exactly ($\sigma_{c2}=3.04$, $\beta_{c2}=0.2692$). We note, however, that our approach works quite well even when σ is chosen relatively far from σ_{c2} and codimension two point conditions are only roughly satisfied.

III. DERIVATION OF THE NONLINEAR ASYMPTOTIC MODEL: INVARIANT-BASED APPROACH

There are two known methods for derivation of the nonlinear dynamical model: (*i*) direct asymptotic approach [6,13] and (*ii*) invariant-based asymptotic approach that involves series expansion of some integral of motion of the analyzed system [4,7]. There is currently some confusion in literature due the fact that so far no comparison has been done between these two procedures. We clarify the situation and demonstrate the complete equivalence between these methods. We show that the first approach makes calculation of linear terms relatively straightforward but computing of nonlinear terms rather complex. In contrast, the invariant-based asymptotic approach allows nonlinear terms to be obtained directly as a result of a Taylor expansion of some conserved quantity of the governing equations. A burdensome part in the implementation of this method is the calculation of certain linear terms. In the next section we use the invariant-based method while an outline of the asymptotic method (which we also use to check our results) is given in Appendix B.

We assume that close to the stability threshold evolution of the soliton parameter β is slow (adiabatic) in Z. This allows us to look for localized solutions of Eqs. (1) in the form of the asymptotic series,

$$U_p(X,Z)=U_s[X,\beta(z)]+\sum_{n=1}^{+\infty}\varepsilon^n U_n(X,z),$$
$$W_p(X,Z)=W_s[X,\beta(z)]+\sum_{n=1}^{+\infty}\varepsilon^n W_n(X,z), \tag{3}$$

where the parameter ε measures smallness of deviation from a stationary soliton (U_s,W_s) and $z=\varepsilon Z$. We are looking for a nonstationary, but localized solution of Eqs. (1) and thus consider only localized functions U_n,W_n. Below we often refer to this nonstationary asymptotic solution as *perturbed* soliton (U_p,W_p).

The substitution of series (3) into the system (1) allows us to calculate consequent orders of (U_p,W_p) in an algorithmic procedure.

Denoting all nonderivative terms of Eqs. (1) as,

$$F_1(U,W,U^*,W^*)\equiv-\beta U+\left(\frac{1}{9}|U|^2+2|W|^2\right)U+\frac{1}{3}U^{*2}W, \tag{4}$$

$$F_2(U,W,U^*,W^*)\equiv-\sigma(3\beta+\Delta)W+(9|W|^2+2|U|^2)W+\frac{1}{9}U^3,$$

we define two linear operators $\hat{L}_I$ and $\hat{L}_R$,

$$\hat{L}_R\equiv\begin{pmatrix}\frac{\partial^2}{\partial X^2}+\frac{\partial F_1}{\partial W}+\frac{\partial F_1}{\partial W^*} & \frac{\partial F_1}{\partial W}+\frac{\partial F_1}{\partial W^*}\\ \frac{\partial F_2}{\partial U}+\frac{\partial F_2}{\partial U^*} & \frac{\partial^2}{\partial X^2}+\frac{\partial F_2}{\partial W}+\frac{\partial F_2}{\partial W^*}\end{pmatrix},$$

$$\hat{L}_I\equiv\begin{pmatrix}\frac{\partial^2}{\partial X^2}+\frac{\partial F_1}{\partial U}-\frac{\partial F_1}{\partial U^*} & \frac{\partial F_1}{\partial W}-\frac{\partial F_1}{\partial W^*}\\ \frac{\partial F_2}{\partial U}-\frac{\partial F_2}{\partial U^*} & \frac{\partial^2}{\partial X^2}+\frac{\partial F_2}{\partial W}-\frac{\partial F_2}{\partial W^*}\end{pmatrix},$$

where all partial derivatives are calculated at (U_s,W_s). For the case of Hamiltonian system (1), operators $\hat{L}_I$ and $\hat{L}_R$ are self-adjoint. Now we are able to present major results of the asymptotic approach in a reasonably compact form.

Substitution of the series (3) into system (1) and collection of the terms of the zero order in ε simply allows us to obtain the system of nonlinear ordinary differential equations for stationary solitons (U_s,W_s). The first-order terms are given by a solution of the following system of *linear* inhomogeneous differential equations,

$$\hat{L}_I\begin{pmatrix}U_1\\W_1\end{pmatrix}=-i\dot{\beta}\begin{pmatrix}U_{s\beta}\\ \sigma W_{s\beta}\end{pmatrix}, \tag{5}$$

where subscript β stands for the derivative with respect to β. System (5) has a localized solution only if its right-hand side is orthogonal to all localized solutions of the corresponding homogeneous system. In particular, it should be orthogonal to the even neutral mode of operator $\hat{L}_I$ that is given by $(U_s,3W_s)$. This orthogonality condition leads to the well-known VK criterion [8], which may be used to find stability threshold point(s) at β_{VK}.

Presenting the first-order terms in the form

$$\begin{pmatrix}U_1\\W_1\end{pmatrix}=i\dot{\beta}\begin{pmatrix}U_{11}\\W_{11}\end{pmatrix}, \tag{6}$$

we proceed to the second-order of our asymptotic approach, calculating the second order correction (U_2,W_2), defined by

$$\hat{L}_R\begin{pmatrix}U_2\\W_2\end{pmatrix}=\ddot{\beta}\begin{pmatrix}U_{11}\\ \sigma W_{11}\end{pmatrix}+\dot{\beta}^2\begin{pmatrix}\partial U_{11}/\partial\beta\\ \sigma\partial W_{11}/\partial\beta\end{pmatrix}-\dot{\beta}^2\begin{pmatrix}U_{11}^2(U_s/9-W_s/3)+2U_sU_1W_{11}/3+2U_sW_{11}^2\\ U_{11}^2(2W_s-U_s/3)+9W_sW_{11}^2\end{pmatrix}. \tag{7}$$

The second-order terms (U_2, W_2) do not impose any nontrivial compatibility conditions and may be presented in the form

$$\begin{pmatrix} U_2 \\ W_2 \end{pmatrix} = \dot{\beta}^2 \begin{pmatrix} U_{21} \\ W_{21} \end{pmatrix} + \ddot{\beta} \begin{pmatrix} U_{22} \\ W_{22} \end{pmatrix}. \tag{8}$$

Proceeding further in a similar way we obtain the following form for the third-order approximation,

$$\begin{pmatrix} U_3 \\ W_3 \end{pmatrix} = i\dot{\beta}^3 \begin{pmatrix} U_{31} \\ W_{31} \end{pmatrix} + i\dot{\beta}\ddot{\beta} \begin{pmatrix} U_{32} \\ W_{32} \end{pmatrix} + i\dddot{\beta} \begin{pmatrix} U_{33} \\ W_{33} \end{pmatrix}, \tag{9}$$

where terms (U_{3i}, W_{3i}), $i=1,2,3$ are solutions of some inhomogeneous differential equations involving operator $\hat{L}_I$ (see Appendix A). As all other odd order terms, the third-order correction (U_3, W_3) impose some nontrivial orthogonality conditions, which we assume to be approximately satisfied. (These conditions in fact require that codimension two point is close enough in the corresponding parameter space.) The terms of the fourth and higher order may be calculated in a similar way, but are not essential for the invariant-based approach used here. Thus we truncate the expression for the adiabatically evolving localized soliton as

$$\begin{pmatrix} U_p \\ W_p \end{pmatrix} = \begin{pmatrix} U_s \\ W_s \end{pmatrix} + i\varepsilon\dot{\beta} \begin{pmatrix} U_{11} \\ W_{11} \end{pmatrix} + \varepsilon^2\dot{\beta}^2 \begin{pmatrix} U_{21} \\ W_{21} \end{pmatrix} + \varepsilon^2\ddot{\beta} \begin{pmatrix} U_{22} \\ W_{22} \end{pmatrix} + i\varepsilon^3 \left[\dot{\beta}^3 \begin{pmatrix} U_{31} \\ W_{31} \end{pmatrix} + 2\dot{\beta}\ddot{\beta} \begin{pmatrix} U_{32} \\ W_{32} \end{pmatrix} + \dddot{\beta} \begin{pmatrix} U_{33} \\ W_{33} \end{pmatrix} \right]. \tag{10}$$

As the next step we construct the Lyapunov functional $L = H + \beta Q$, where Hamiltonian H and energy Q are given by expressions (2).

Substituting the series (3) into the functional L and keeping terms up to the fourth order in ε we obtain

$$\begin{aligned} L &= H_p + \beta Q_p \\ &= H_s + \beta Q_s + \varepsilon^2 \frac{1}{2} D_1 \dot{\beta}^2 \\ &\quad + \varepsilon^4 \left[\frac{1}{2} D_2 (2\dot{\beta}\ \dddot{\beta} - \ddot{\beta}^2) + \dot{\beta}^4 A + \dot{\beta}^2 \ddot{\beta} B \right], \end{aligned} \tag{11}$$

where H_p, Q_p stand for the values of the invariants calculated for the perturbed (nonstationary) asymptotic solution (10), H_s, Q_s are invariants calculated for the stationary soliton solutions (U_s, W_s), coefficients D_i have the same definitions as in [13]:

$$\begin{aligned} D_1(\beta) &= -2\langle (U_{11}, W_{11}) | \hat{L}_I (U_{11}, W_{11}) \rangle, \\ D_2(\beta) &= -2\langle (U_{33}, W_{33}) | \hat{L}_I (U_{11}, W_{11}) \rangle \\ &= 2\langle (U_{22}, W_{22}) | \hat{L}_R (U_{22}, W_{22}) \rangle, \end{aligned} \tag{12}$$

where $\langle \mathbf{U} | \mathbf{W} \rangle \equiv \Sigma_i \int dX U_i W_i^*$. The coefficients A and B are also given by similar overlap integrals, but we do not present their specific structure here.

To simplify the expression (11) we introduce the variable $\delta\beta \equiv \beta - \beta_0$, where soliton parameter β_0 is given by the equation $Q_s(\beta_0) = Q_p$. To go further we define two more coefficients

$$D_0(\beta_0) = \left. \frac{\partial Q}{\partial \beta} \right|_{\beta_0}, \quad \gamma(\beta_0) = \frac{1}{2} \left. \frac{\partial^2 Q}{\partial \beta^2} \right|_{\beta_0}. \tag{13}$$

In the vicinity of codimension two bifurcation the following assumptions for coefficients D_i are essential: $D_0 = \varepsilon^4 \tilde{D}_0$, $D_1 = \varepsilon^2 \tilde{D}_1$, $D_{i \geq 2} \sim O(1)$, (see Ref. [13]). Assuming that $\delta\beta = \varepsilon^4 \delta\tilde{\beta}$, expanding all functionals in L in the Taylor series around β_0, and keeping terms up to the ε^{12} we obtain

$$\begin{aligned} H_p = H_0(\beta_0) + \varepsilon^{12} \Big[&\frac{1}{2} D_1 \delta\dot{\beta}^2 + \frac{1}{2} D_2 (2\delta\dot{\beta}\delta\dddot{\beta} - \delta\ddot{\beta}^2) \\ &+ \frac{1}{2} D_0 \delta\beta^2 + \frac{1}{3} \gamma \delta\beta^3 \Big], \end{aligned} \tag{14}$$

where all tildes are omitted for brevity.

Introducing canonical variables (q_1, q_2, p_1, p_2)

$$\begin{aligned} q_1 &= \delta\beta, \\ q_2 &= -\delta\dot{\beta}, \\ p_1 &= D_2 \delta\ddot{\beta} + D_1 \delta\dot{\beta}, \\ p_2 &= D_2 \delta\ddot{\beta}, \end{aligned} \tag{15}$$

we transform the function in the square brackets of the expression (14) to the classical Hamiltonian form:

$$\tilde{H} = -p_1 q_2 - \frac{1}{2D_2} p_2^2 + \frac{1}{2} D_0 q_1^2 + \frac{1}{3} \gamma q_1^3 - \frac{1}{2} D_1 q_2^2. \tag{16}$$

Dynamical equations for this system have the form

$$\begin{aligned} \dot{q}_1 &= -q_2, \\ \dot{q}_2 &= -\frac{1}{D_2} p_2, \\ \dot{p}_1 &= -D_0 q_1 - \gamma q_1^2, \end{aligned} \tag{17}$$

$$\dot{p}_2 = p_1 + D_1 q_2 .$$

After back substitution of the definitions (15), the system of equation (17) may be presented as

$$D_2 \delta \dddot{\beta} + D_1 \delta \ddot{\beta} + D_0 \delta\beta + \gamma \delta\beta^2 = 0. \tag{18}$$

Nonlinear ODE (18) describes adiabatic evolution of the soliton parameter β ($\equiv \beta_0 + \delta\beta$) in the vicinity of the VK and oscillatory instability thresholds. Due to local one-to-one correspondence between the soliton solution and its internal parameter, model (18) indirectly describes adiabatic evolution of a weakly perturbed soliton.

An alternative derivation of Eq. (18) may be found in Appendix B. The structure of equation (18) is generic for Hamiltonian systems with phase-translational symmetry. Coefficients D_0, D_1, and D_2 measure orthogonality between the corresponding symmetry-induced neutral mode and perturbations of the first lowest orders, γ characterizes dependence of the corresponding conserved quantity (energy) from the corresponding internal parameter. A linear version of Eq. (18) was obtained in Ref. [13]. Among other major conclusions that can be obtained from analysis of Eq. (18) is the expression for the oscillatory instability threshold at β_{os} that is given implicitly by the equation

$$D_1^2 - 4 D_0 D_2 = 0. \tag{19}$$

IV. ANALYSIS OF THE NONLINEAR EVOLUTION MODEL

A. Calculation of the coefficients

Analysis of the nonlinear model starts from the calculation of the coefficients in Eq. (18). Computing of the coefficients D_0 and γ is direct. Expressions for other coefficients involve computation of different order terms in the series (3). In particular, calculation of the coefficient D_1 (which is often referred to as a *mass* coefficient) includes numerical resolution of the problem

$$\hat{L}_I \begin{pmatrix} U_{11} \\ W_{11} \end{pmatrix} = - \begin{pmatrix} U_{s\beta} \\ \sigma W_{s\beta} \end{pmatrix}. \tag{20}$$

The general solution of Eqs. (20) is a sum of the solution of the corresponding homogeneous problem and the particular solution of the inhomogeneous problem itself: $(U_{11}, W_{11})_g = (U_{11}, W_{11})_p + C(U_s, 3W_s)$, C is an arbitrary constant. For our purposes we only need the $(U_{11}, W_{11})_p$ part. In theoretical consideration the contribution $C(U_s, 3W_s)$ can be eliminated by simply taking $C=0$. However, numerical separation of two parts (both of even symmetry) of the localized solution $(U_{11}, W_{11})_g$ may be a challenging task (singular ODE problem). This separation is necessary indeed, because the solvability condition for the calculation of the first-order terms in the series (10) only demands the *approximate* orthogonality of $(U_{s\beta}, W_{s\beta})$ to the neutral mode of the operator $\hat{L}_I$, i.e., to $(U_s, 3W_s)$, and thus any small deviation of β_0 from VK point β_{VK} may lead to nontrivial and uncontrollable contributions to D_1 coefficient due to $C(U_s, 3W_s)$ term.

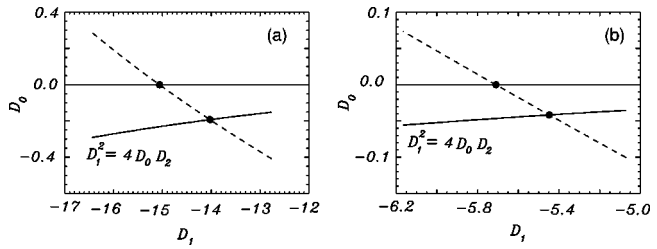

FIG. 4. Dependence D_0 versus D_1 (dashed line) in the neighborhood of stationary and oscillatory instability thresholds (solid lines) plotted for $\sigma = 2.5$, (a), and $\sigma = 2.8$, (b).

To expel this part from the general solution we use a homotopy method. We introduce a continuous parameter s and construct a linear operator family $\hat{L}(s) = s\hat{L}_I + (1-s)\hat{L}_R$. The generalized problem (20) with operator $\hat{L}_I$ replaced by $\hat{L}(s)$ is singular only at $s=1$, where even localized solution of the corresponding homogeneous problem exists. Numerically this singularity manifests itself in a small vicinity around $s=1$. Replacing the solution of the generalized inhomogeneous problem in the singular region by the interpolation of the solutions from the neighboring regular regions we obtain $(U_{11}, W_{11})_p$ at $s=1$ with a high accuracy.

Coefficient D_2 can be calculated in a standard (nonsingular) way provided the right-hand side of the Eq. $\hat{L}_R(U_{22}, W_{22}) = (U_{11}, \sigma W_{11})$ is even in X and automatically orthogonal to the neutral (zero eigenvalue) eigenmode $(\partial U_s/\partial X, \partial W_s/\partial X)$ of operator $\hat{L}_R$. Figure 4 represents results of calculation of the D_i, $i=0,1,2$ in the vicinity of VK instability ($D_0 = 0$) and oscillatory instability thresholds ($D_1^2 = 4 D_0 D_2$) for two representative values of σ. Note that, for our model, D_1 (mass coefficient) is *negative* in the vicinity of VK and oscillatory instability thresholds at $\sigma \sim 3$.

B. Linear limit

To check accuracy of the asymptotic model (18) we calculated the spectrum of the linearized (about stationary solitons) version of system (1) in the vicinity of the stability window. Strictly speaking, system (1) is Galilean invariant only at $\sigma = 3.0$ when instability development due to bifurcation from the antisymmetric neutral mode $(\partial U_s/\partial X, \partial W_s/\partial X)$ is absent. We assume that this scenario of instability development is absent in the vicinity of $\sigma = 3$ and to avoid excessive difficulties related to smallness of the

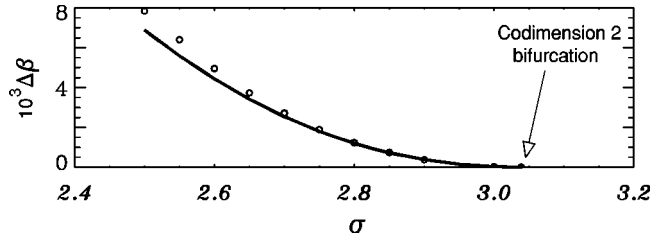

FIG. 5. Size of the stability window versus σ. Solid line corresponds to the theoretical prediction of the model, the circles present the direct numerical results.

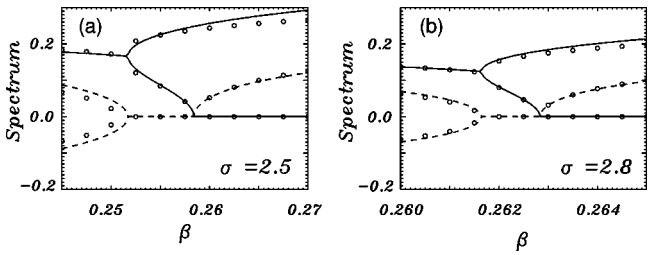

FIG. 6. Linear spectrum of Eq. (1) calculated for $\sigma=2.5$ (a), and $\sigma=2.8$ (b). Solid curves and filled circles correspond to the positive real part of the eigenvalue, dashed curves and open circles, to the imaginary part. All curves are given by the analytic expression (21), the circles represent the direct numerical results.

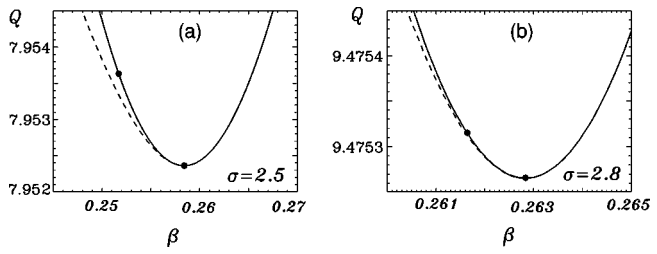

FIG. 7. Energy invariant Q [see Eq. (2)] calculated for the higher-order soliton family of interest versus soliton parameter β (solid curves) and its parabolic approximation (dashed curves) used in the model (18). Filled circles correspond to the instability thresholds. (a) for $\sigma=2.5$, (b) for $\sigma=2.8$.

stability window (Fig. 5) choose a value of the σ for which the stability window is easily detectable.

The model (18) predicts the appearance of quadruplets of complex eigenvalues that are given by the following expression:

$$\lambda^2=\frac{-D_1\pm\sqrt{D_1^2-4D_0D_2}}{2D_2}. \tag{21}$$

The comparison between analytical result (21) and direct numerical computations is presented in Fig. 6 for two cases, $\sigma=2.5$ and $\sigma=2.8$. Our theory correctly predicts both the positions of the stability and oscillatory instability thresholds and the linear spectrum in the vicinity of these thresholds. The agreement is better for the case $\sigma=2.8$ as then the maximal deviation from the codimension two point ($\sigma_{c2}=3.04$, $\beta_{c2}=0.2692$) is smaller.

C. Stationary points

Coefficients in front of the nonlinear terms in the model (18) arise as a result of Taylor expansion of the energy functional near the VK instability threshold. This expansion can result in the inclusion of cubic and other higher-order corrections into the final model (18). Our analysis shows that it is sufficient to include only the quadratic term. Physically, the condition for the truncation of this Taylor series is the adequate description of major characteristic features of the complete nonlinear system. In the case of system (1) this includes the number and type of soliton states achievable for some fixed soliton energy Q_p in the vicinity of β_{VK}. Our model (18) with only the lowest-order nonlinear term correctly predicts the number of stationary points (corresponding to stationary solitons) and their types. Figure 7 shows the reason for this successful behavior demonstrating a rather small deviation between actual dependence of energy invariant calculated on stationary soliton family and the parabolic approximation employed in our model (18).

D. Instability scenarios

Both the previous models (see Refs. [4,6]) and model (18) yield similar predictions for the number and positions of the stationary points for variation of the soliton parameter, namely, $\delta\beta=0,-D_0/\gamma$. The advantage of our model is associated with the increased dimensionality of the phase space of Eq. (18) resulting in broader variety of spectral characteristics and instability development scenarios.

Direct modeling of Eq. (18) is straightforward except for certain difficulties associated with unbounded type of motion demonstrated by this dynamical system. (Bounded trajectories exist only in the vicinity of the stable stationary points.) However, significant physical insight into the behavior of the complete system (1) may be obtained from consideration of the cross sections of the phase diagram corresponding to the four-dimensional phase space of the model (18).

First, let us consider energy Q_p of the perturbed soliton lying in the interval (Q_{vk},Q_{os}), where Q_{vk} and Q_{os} are energies of stationary solitons at the VK and oscillatory instability thresholds, respectively, Fig. 8(a). In this case dynamics of the system is determined by coexistence of the saddle-center fixed point β_{01} and the center β_{f1} that is presented qualitatively in Fig. 8(c). If an initial perturbation of the stationary soliton with β_{01} is ''positive,'' i.e., brings β to the

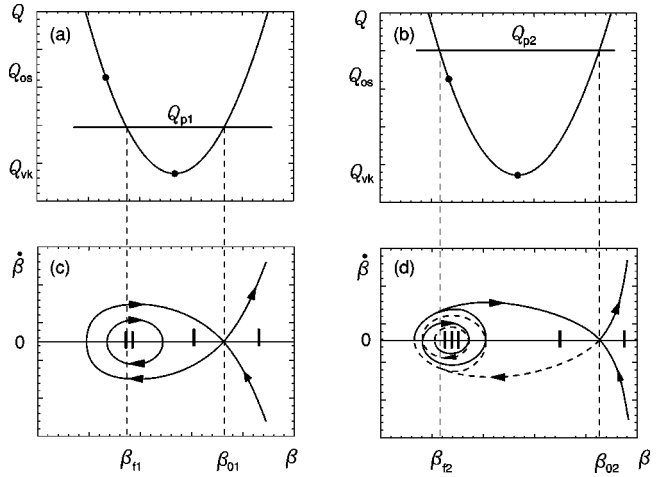

FIG. 8. Qualitative change due to increase of perturbation strength. Left part: (a) smaller perturbation (lower level of Q_p) of a stationary soliton in the vicinity of β_{VK} leads to a phase diagram cross section that includes center and saddle-center fixed points (c). Right part: (b) larger perturbation (higher level of Q_p) leads to a phase diagram cross section that includes unstable spiral and saddle-center fixed points (d). Solid circles stand for the instability thresholds.

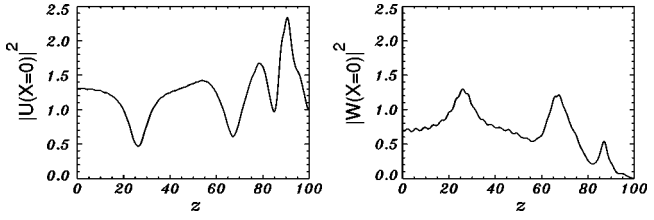

FIG. 9. Unstable stationary soliton with small ''negative'' perturbation. Rapid increase of amplitude with oscillations resulting in decay. $\beta=0.2635$, $\sigma=2.8$.

right of β_{01}, instability development leads to a rapid increase of soliton parameter β, similar to the regime 1 of Fig. 3(b) of Ref. [4]. At the same time presence of an internal mode in this region of β can lead to simultaneous excitation of oscillations. This scenario persists for small ''negative'' initial perturbations, which bring initial β to the left of β_{01}. This regime is *different* from the regime 3 of Fig. 3(b) of Ref. [4] due to presence of an extra degree of freedom in our model — we observe *more than one* large-scale oscillation before rapid increase of β. We note, that due to absence of collapse in system (1) and influence of nonlinear terms beyond the approximation of the model (18) this rapid increase of β evolves into decay (see Fig. 9). In contrast, if an initial negative perturbation $\delta\beta$ puts the system closer to the stable point β_{f1} (region II) the motion of the system becomes almost periodic (see Fig. 10). This regime is similar to the regime 2 of Fig. 3(b) of Ref. [4]. The initial conditions taken in a close vicinity of the stable point β_{f1} results in the phase trajectory lying on the torus corresponding to the beating of two frequencies, (see Fig. 11). There is no analog to this behavior in any previous works.

Scenarios of instability development in the case when energy Q_p of the perturbed soliton is greater then Q_{os} are defined by coexistence of the saddle-center point β_{02} and of the focus β_{f2}, Figure 8(b,d). All observed regimes for this case have no analogs in previous works [4–7]. For small positive deviation $\delta\beta$ from the parameter β_{02} (region I) we again have a few large-scale oscillations that after rapid increase of β evolve into decay of the soliton. If initial perturbation $\delta\beta$ forces transition of the system into a state in vicinity of the focus β_{f2} (region III) initial evolution of the perturbation undergoes oscillatory instability that usually develops into decay (see Fig. 12). However, a confined regime of soliton evolution is also possible for this case. This regime utilize the fact that the stationary point β_{02} may have center-type

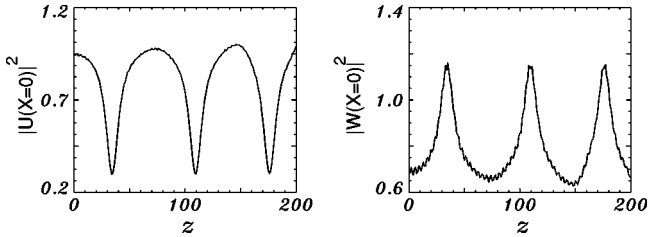

FIG. 10. Unstable stationary soliton with larger ''negative'' perturbation. Longer-term oscillations at $\beta=0.262$, $\sigma=2.5$. Negative initial $\delta\beta$ puts the system into region II in Fig. 8.

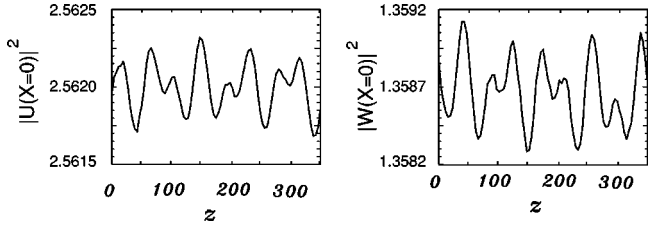

FIG. 11. Perturbed stable stationary soliton. Beating of two frequencies, at $\beta=0.2619$ and $\sigma=2.8$.

cross section and demonstrates a complex quasiperiodic evolution (see Fig. 13).

Note, that to check predictions of model (18), we integrated the system of partial differential equations (PDE) starting from the differently perturbed stationary solitons in the vicinity of VK threshold. Perturbation was taken in the form:

$$\begin{pmatrix}\Delta U\\ \Delta W\end{pmatrix}=a\begin{pmatrix}U_s\\ W_s\end{pmatrix}+b\begin{pmatrix}\partial^2U_s/\partial X^2\\ \partial^2W_s/\partial X^2\end{pmatrix}+c\begin{pmatrix}\partial^4U_s/\partial X^4\\ \partial^4W_s/\partial X^4\end{pmatrix}+d\begin{pmatrix}\partial^6U_s/\partial X^6\\ \partial^6W_s/\partial X^6\end{pmatrix},\tag{22}$$

where a, b, c, and d define the perturbation. [We need four coefficients to define the perturbation in order to span four-dimensional phase space of Eq. (18).] Other choices of four perturbation functions are possible.

V. CONCLUSION AND DISCUSSION

In conclusion, we have developed a theory describing longer-term nonlinear dynamics of perturbed higher-order solitons in the vicinity of codimension two point. It was shown that for a large range of instability scenarios that could not be analyzed in the frame of previously known nonlinear models our theory successfully describes higher-order soliton perturbation-induced dynamics. For the thoroughly investigated example of solitons due to degenerate FWM our theory predicts correctly the linear spectrum of perturbation (instability threshold positions, instability rates),

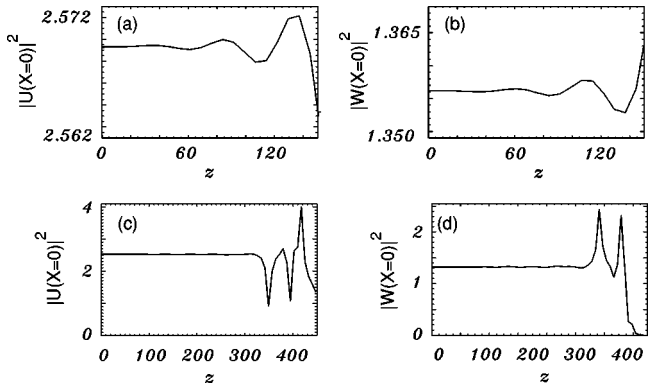

FIG. 12. Perturbed oscillatory unstable stationary soliton. Oscillatory instability at $\beta=0.2667$ and $\sigma=2.8$. (a),(b) initial stage; (c),(d) longer-scale behavior.

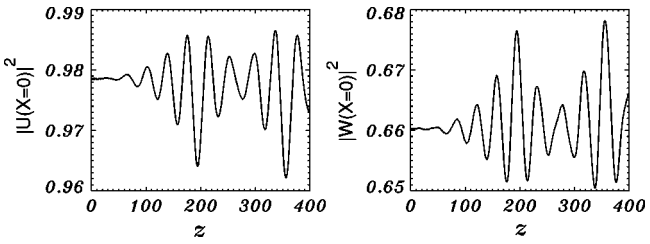

FIG. 13. Perturbed oscillatory unstable stationary soliton. Confined oscillatory instability at $\beta=0.25$ and $\sigma=2.5$. Negative initial $\delta\beta$.

and types of stationary points as well as various scenarios for longer-term soliton evolution. In general, we have completed the missing link between codimension one point weakly nonlinear approaches of Refs. [6,4] and codimension two point linear theory of Ref. [13].

The two-fold derivation of the nonlinear model has demonstrated complete equivalence between asymptotic and invariant-based approaches leading to two alternative interpretations of the resulting coefficients. The structure of the nonlinear model suggests that our results may be readily applied to other nonlinear models of different physical content. In practice, our theory may be used to describe perturbed higher-order soliton dynamics (in, or close to, their stability windows) if more conventional approaches fail in this region of system parameters.

The major difference between our model (18) and previously developed one-parameter soliton evolution models is in increased dimensionality of model phase space. In fact Eq. (18) is a nonlinear Hamiltonian system with two degrees of freedom. Thus, it is almost certainly a *chaotic* system [16]. For the particular case of parameter values in Eq. (18) associated with degenerate FWM solitons studied in this paper chaotical motion characteristics are hard to analyze because the corresponding dynamical trajectories are typically unbounded, but this can differ for other physical models where our theory is applicable. The challenge is to identify such soliton systems.

Another interesting direction of further activity is in generalization of our results to multi-parameter soliton systems (e.g., with two or more β-like parameters). Promising candidates for the corresponding physical example are not fully degenerate parametric four-wave-mixing models.

ACKNOWLEDGMENT

D.V.S. acknowledges support from the Royal Society of Edinburgh and UK EPSRC Grant No. GR/N19830.

APPENDIX A: THIRD-ORDER TERMS FOR THE INVARIANT-BASED APPROACH

Components of the third-order approximation (9) can be found from the following differential equations:

$$\hat{L}_I\begin{pmatrix} U_{31} \\ W_{31}\end{pmatrix}=-\begin{pmatrix} \partial U_{21}/\partial\beta+U_1^3/9-U_1^2W_1/3+2U_sU_{21}W_1/3 \\ \sigma\partial W_{21}/\partial\beta-U_1^3/9+2U_sU_1U_{21}/3\end{pmatrix}-\begin{pmatrix} 2U_1W_1^2+2U_1[U_{21}(U_s-3W_s)-6W_{21}(U_s-6W_s)]/9 \\ 2U_1^2W_1+9W_1^3+2W_1(2U_sU_{21}+9W_sW_{21})\end{pmatrix},$$

$$\hat{L}_I\begin{pmatrix} U_{32} \\ W_{32}\end{pmatrix}=-\begin{pmatrix} 2U_{21}+\partial U_{22}/\partial\beta \\ 2W_{21}+\sigma\partial W_{22}/\partial\beta\end{pmatrix}-\frac{2}{3}\begin{pmatrix} U_sU_{22}W_1+U_1[U_{22}(U_s/3-W_s)-U_sW_{22}] \\ U_sU_1U_{22}+3W_1(2U_sU_{22}+9W_sW_{22})\end{pmatrix},$$

$$\hat{L}_I\begin{pmatrix} U_{33} \\ W_{33}\end{pmatrix}=-\begin{pmatrix} U_{22} \\ \sigma W_{22}\end{pmatrix}.$$

APPENDIX B: ASYMPTOTIC APPROACH

We assume that close to the stability threshold the phase shift β varies adiabatically with distance z and the variation of it $\delta\beta=\beta-\beta_0$ is small, where β_0 is taken in the vicinity of VK stability threshold. We look for solutions in the form

$$U(X,Z)=u(X,z;\beta)e^{i\varepsilon^3\int_0^z\delta\beta(t)dt},$$

$$W(X,Z)=w(X,z;\beta)e^{3i\varepsilon^3\int_0^z\delta\beta(t)dt},$$

$$z=\varepsilon Z,\quad \varepsilon\ll 1, \tag{B1}$$

and obtain the following system of equations

$$\frac{\partial^2u}{\partial x^2}+F_1(u,w,u^*,w^*)=\varepsilon^4\delta\beta u-i\varepsilon u_z,$$

$$\frac{\partial^2w}{\partial x^2}+F_2(u,w,u^*,w^*)=3\varepsilon^4\delta\beta w-i\varepsilon\sigma w_z, \tag{B2}$$

where F_1 and F_2 are given similar to Eq. (4) definitions.

There are two ways to proceed with the asymptotic approach: (i) to add a pair of equations complex conjugate to the system (B2) and work with vectors (u,w,u^*,w^*) as in Ref. [13], (ii) or to separate complex functions (u,w) into real and imaginary parts and work with vectors (u_R,w_R,u_I,w_I). Below we adopted the second approach.

We expand the solution to Eqs. (B2) into an asymptotic series:

$$u = u_s + \varepsilon^4 u_4 + i\varepsilon^5 u_5 + \varepsilon^6 u_6 + \cdots,$$
$$w = w_s + \varepsilon^4 w_4 + i\varepsilon^5 w_5 + \varepsilon^6 w_6 + \cdots. \tag{B3}$$

Here we already take into account the structure of Eqs. (B2) explicitly omitting first three trivial (zero) orders. Also at $\sigma = 3$ the system (1) is Galilean invariant. As a result at $\sigma = 3$ the stability of stationary waves cannot be lost due to VK-like bifurcation from an antisymmetric neutral mode $(\partial u_s/\partial X, \partial w_s/\partial X)$ of linear spectrum. We assume that this property stays for $\sigma \simeq 3$ and only consider perturbations belonging to the class of symmetric functions. This assumption ensures that all consecutive even order corrections in series (B3) are purely real, whereas all odd order corrections are purely imaginary. This, in turn, allows us to work with 2×2 matrix operators, instead of 4×4 operators.

Linearization of functions F_1, F_2 about real stationary solution (u_s, w_s) yields linear self-adjoint operators $\hat{M}_I$ and $\hat{M}_R$,

$$\hat{M}_R = \begin{pmatrix} \dfrac{\partial^2}{\partial X^2} + \dfrac{\partial F_1}{\partial u} + \dfrac{\partial F_1}{\partial u^*} & \dfrac{\partial F_1}{\partial w} + \dfrac{\partial F_1}{\partial w^*} \\ \dfrac{\partial F_2}{\partial u} + \dfrac{\partial F_2}{\partial u^*} & \dfrac{\partial^2}{\partial X^2} + \dfrac{\partial F_2}{\partial w} + \dfrac{\partial F_2}{\partial w^*} \end{pmatrix},$$

$$\hat{M}_I = \begin{pmatrix} \dfrac{\partial^2}{\partial X^2} + \dfrac{\partial F_1}{\partial u} - \dfrac{\partial F_1}{\partial u^*} & \dfrac{\partial F_1}{\partial w} - \dfrac{\partial F_1}{\partial w^*} \\ \dfrac{\partial F_2}{\partial u} - \dfrac{\partial F_2}{\partial u^*} & \dfrac{\partial^2}{\partial X^2} + \dfrac{\partial F_2}{\partial w} - \dfrac{\partial F_2}{\partial w^*} \end{pmatrix},$$

with all partial derivatives taken at stationary soliton solution (u_s, w_s) that is obtained in the zero order in ε. The next, three-order corrections are trivial (zero) as we have already mentioned above. Solution of the next, fourth-order approximation is given by the system

$$\hat{M}_R \begin{pmatrix} u_4 \\ w_4 \end{pmatrix} = \delta\beta \begin{pmatrix} u_s \\ 3\sigma w_s \end{pmatrix}, \tag{B4}$$

and may be found exactly as

$$\begin{pmatrix} u_4 \\ w_4 \end{pmatrix} = \delta\beta \begin{pmatrix} u_{s\beta} \\ w_{s\beta} \end{pmatrix}. \tag{B5}$$

Proceeding further we obtain

$$\hat{M}_I \begin{pmatrix} u_5 \\ w_5 \end{pmatrix} = -\delta\dot{\beta} \begin{pmatrix} u_{s\beta} \\ \sigma w_{s\beta} \end{pmatrix}. \tag{B6}$$

In this order we have the nontrivial solvability condition that is approximately satisfied if the stationary soliton of zero-order approximation (u_s, w_s) is chosen in the vicinity of the VK stability threshold. Presenting the fifth-order correction in the form

$$\begin{pmatrix} u_5 \\ w_5 \end{pmatrix} = \delta\dot{\beta} \begin{pmatrix} u_{51} \\ w_{51} \end{pmatrix}, \tag{B7}$$

we can proceed with the sixth-order correction,

$$\hat{M}_R \begin{pmatrix} u_6 \\ w_6 \end{pmatrix} = \delta\ddot{\beta} \begin{pmatrix} u_{51} \\ \sigma w_{51} \end{pmatrix}, \tag{B8}$$

which we present in the form

$$\begin{pmatrix} u_6 \\ w_6 \end{pmatrix} = \delta\ddot{\beta} \begin{pmatrix} u_{61} \\ w_{61} \end{pmatrix}. \tag{B9}$$

Note that odd order corrections do not impose any nontrivial compatibility conditions. Next order terms may be found from

$$\hat{M}_I \begin{pmatrix} u_7 \\ w_7 \end{pmatrix} = -\delta\dddot{\beta} \begin{pmatrix} u_{61} \\ \sigma w_{61}. \end{pmatrix}. \tag{B10}$$

Again, as in all odd orders, we need to satisfy certain orthogonality conditions. At this stage we just assume that these conditions are approximately satisfied and present seventh-order correction as

$$\begin{pmatrix} u_7 \\ w_7 \end{pmatrix} = \delta\dddot{\beta} \begin{pmatrix} u_{71} \\ w_{71} \end{pmatrix}. \tag{B11}$$

First contribution from the nonlinear terms of Eqs. (B2) to the asymptotic expansion appears in the eighth order,

$$\hat{M}_R\begin{pmatrix} u_8 \\ w_8 \end{pmatrix} = \delta\dddot{\beta}\begin{pmatrix} u_{71} \\ \sigma w_{71} \end{pmatrix} + \delta\beta^2\begin{pmatrix} u_{s\beta} - 2u_s w_{s\beta}^2 \\ 3\sigma w_{s\beta} - 27 w_s w_{s\beta}^2 \end{pmatrix} - \delta\beta^2\begin{pmatrix} \frac{1}{3}(u_s + w_s)u_{s\beta}^2 + (\frac{2}{3}u_s + 4w_s)u_{s\beta}w_{s\beta} \\ (\frac{1}{3}u_s + 2w_s)u_{s\beta}^2 + 4u_s u_{s\beta} w_{s\beta} \end{pmatrix}. \tag{B12}$$

Solution due to the terms with $\delta\beta^2$ factor can be calculated analytically. This allows us to present the eighth-order terms in the form:

$$\begin{pmatrix} u_8 \\ w_8 \end{pmatrix} = \delta\dddot{\beta}\begin{pmatrix} u_{81} \\ w_{81} \end{pmatrix} + \frac{1}{2}\delta\beta^2\begin{pmatrix} u_{s\beta\beta} \\ w_{s\beta\beta} \end{pmatrix}. \tag{B13}$$

Proceeding to the ninth order we obtain

$$\hat{M}_I\begin{pmatrix} u_9 \\ w_9 \end{pmatrix} = -\delta\beta^{(V)}\begin{pmatrix} u_{81} \\ \sigma w_{81} \end{pmatrix} - \delta\beta\delta\dot{\beta}\begin{pmatrix} u_{s\beta\beta} \\ \sigma w_{s\beta\beta} \end{pmatrix} - \delta\beta\delta\dot{\beta}\begin{pmatrix} \frac{2}{3}u_s u_{s\beta} w_{51} - u_{51} \\ 4u_s u_{s\beta} w_{51} - 3\sigma w_{51} \end{pmatrix}$$

$$- \delta\beta\delta\dot{\beta}\begin{pmatrix} (\frac{2}{9}u_s - \frac{2}{3}w_s)u_{s\beta}u_{51} + (4w_s - \frac{2}{3}u_s)u_{51}w_{s\beta} \\ 18 w_s w_{s\beta} w_{51} + \frac{2}{3}u_s u_{s\beta} u_{51} \end{pmatrix}. \tag{B14}$$

Now we use a *combined* solvability condition for all odd orders we considered [which requires that the sum of right-hand-side parts of the systems (B6),(B10),(B14) should be orthogonal to the neutral mode of $\hat{M}_I$ operator $(u_s, 3w_s)$] obtaining

$$D_2\delta\beta^{(V)} + D_1\delta\dddot{\beta} + D_0\delta\dot{\beta} + 2\gamma\delta\beta\delta\dot{\beta} = 0, \tag{B15}$$

where

$$D_2 = 2\int_{-\infty}^{+\infty}(u_0 u_{81} + 3\sigma w_0 w_{81})\ dx, \tag{B16}$$

$$D_1 = 2\int_{-\infty}^{+\infty}(u_0 u_{61} + 3\sigma w_0 w_{61})\ dx,$$

$$D_0 = 2\int_{-\infty}^{+\infty}(u_0 u_{0\beta} + 3\sigma w_0 w_{0\beta})\ dx,$$

$$\gamma = \frac{1}{2}\left.\frac{\partial^2 Q}{\partial\beta^2}\right|_{\beta_0}.$$

It may be shown that all coefficients (B16) are identically equal to the corresponding coefficients (12) and (13). After one integration of Eq. (B15) in z and putting the integration constant to zero we obtain the model describing nonlinear soliton dynamics in the vicinity of the stability threshold:

$$D_2\delta\ddot{\beta} + D_1\delta\ddot{\beta} + D_0\delta\beta + \gamma\delta\beta^2 = 0. \tag{B17}$$

This equation is identical to the model (18).

[1] M. Segev and G. I. Stegeman, Phys. Today **51**(8), 42 (1998), and references therein; G. I. Stegeman, D. J. Hagan, and L. Torner, Opt. Quantum Electron. **28**, 1691 (1996).

[2] W. E. Torruellas *et al.*, Phys. Rev. Lett. **74**, 5036 (1995); J. U. Kang *et al.*, *ibid.* **76**, 3699 (1996); H. S. Eisenberg *et al.*, *ibid.* **81**, 3383 (1998); B. Bourliaguet *et al.*, Opt. Lett. **24**, 1410 (1999).

[3] E. A. Kuznetsov, A. M. Rubenchik, and V. E. Zakharov, Phys. Rep. **142**, 103 (1986); M. Grillakis, J. Shatah, and W. Strauss, J. Funct. Anal. **94**, 308 (1990); R. L. Pego and M. I. Weinstein, Commun. Math. Phys. **164**, 305 (1994); Y. A. Li and K. Promislow, Physica D **124**, 137 (1998); D. E. Pelinovsky and Yu. S. Kivshar, Phys. Rev. E **62**, 8668 (2000).

[4] D. E. Pelinovsky, V. V. Afanasjev, and Y. S. Kivshar, Phys. Rev. E **53**, 1940 (1996).

[5] V. I. Karpman and A. G. Shagalov, Physica D **144**, 194 (2000).

[6] D. E. Pelinovsky, A. V. Buryak, and Y. S. Kivshar, Phys. Rev. Lett. **75**, 591 (1995).

[7] A. V. Buryak, Y. S. Kivshar, and S. Trillo, Phys. Rev. Lett. **77**, 5210 (1996).

[8] N. G. Vakhitov and A. A. Kolokolov, Radiophys. Quantum Electron. **16**, 783 (1973).

[9] T. Peschel *et al.*, Phys. Rev. E **55**, 4730 (1997); W. C. K. Mak, B. A. Malomed, and P. L. Chu, *ibid.* **58**, 6708 (1998); E. A. Ostrovskaya *et al.*, Phys. Rev. Lett. **83**, 296 (1999); Z. H. Musslimani *et al.*, *ibid.*, **84**, 1164 (2000); J. J. García-Ripoll *et al.*, *ibid.* **85**, 82 (2000); T. Carmon *et al.*, Opt. Lett. **25**, 1113 (2000); W. Krolikowski *et al.*, Phys. Rev. Lett. **85**, 1424 (2000).

[10] K. Y. Kolossovski, A. V. Buryak, and R. A. Sammut, Phys. Lett. A ; **279**, 355 (2001).

[11] H. T. Tran, J. D. Mitchell, N. N. Akhmediev, and A. Ankiewicz, Opt. Commun. **93**, 227 (1992); N. Akhmediev, A.

Ankiewicz, and H. T. Tran, J. Opt. Soc. Am. B **10**, 230 (1993).
[12] I. V. Barashenkov, D. E. Pelinovsky, and E. V. Zemlyanaya, Phys. Rev. Lett. **80**, 5117 (1998); D. V. Skryabin and W. J. Firth, Phys. Rev. E **58**, R1252 (1998); D. Mihalache, D. Mazilu, and L. Torner, Phys. Rev. Lett. **81**, 4353 (1998).
[13] D. V. Skryabin, Physica D **139**, 186 (2000).
[14] D. Liu and H. G. Winful, Opt. Lett. **16**, 67 (1991); L. M. Kovachev, Opt. Quantum Electron. **24**, 55 (1992); N. A. Ansari, R. A. Sammut, and H. T. Tran, J. Opt. Soc. Am. B **13**, 1419 (1996); **14**, 298 (1997).
[15] P. B. Lundquist, D. R. Andersen, and Y. S. Kivshar, Phys. Rev. E **57**, 3551 (1998); R. A. Sammut, A. V. Buryak, and Y. S. Kivshar, J. Opt. Soc. Am. B **15**, 1488 (1998); K. Y. Kolossovski *et al.*, Phys. Rev. E **62**, 4309 (2000).
[16] A. J. Lichtenberg and M. A. Lieberman, *Regular and Chaotic Dynamics* (Springer, New York, 1992).